Technical Notes and Correspondence

Information Centrality and Ordering of Nodes for Accuracy in Noisy Decision-Making Networks

Ioannis Poulakakis, *Member, IEEE*, George F. Young, *Member, IEEE*, Luca Scardovi, *Member, IEEE*, and Naomi Ehrich Leonard, *Fellow, IEEE*

***Abstract*—This technical note considers a network of stochastic evidence accumulators, each represented by a drift-diffusion model accruing evidence towards a decision in continuous time by observing a noisy signal and by exchanging information with other units according to a fixed communication graph. These network dynamics model distributed sequential hypothesis testing as well as collective decision making. We prove the relationship between the location of each unit in the graph and its certainty as measured by the inverse of the variance of its state. Under mild connectivity assumptions, we show that only in balanced directed graphs do the node variances remain within a bounded constant from the minimum possible variance. We then prove that, for these digraphs, node ranking based on certainty is governed by information centrality, which depends on the notion of effective resistance suitably generalized to directed graphs. Our results, which describe the certainty of each unit as a function of the structural properties of the graph, can guide the selection of leaders in problems that involve the observation of noisy external signals by a cooperative multi-agent network.**

***Index Terms*—Decision making, distributed hypothesis testing, drift diffusion, information centrality, leader selection, noisy networks.**

I. Introduction

The identification of the most certain units in a network of sensors accumulating evidence by observing noisy processes is central to shaping collective behavior. The contribution of the present technical note is to rigorously characterize the impact of the communication graph on the certainty—i.e., accuracy—of each unit in a decision-making network of stochastic evidence accumulators.

In decision making, evidence accumulation often assumes that relevant information is collected sequentially, through a series of independent scalar observations. This assumption forms the basis for a large class of decision-making tests, including Wald's Sequential Probability Ratio Test (SPRT) and its variations [1]. In the classical two-choice SPRT test, the information accrued by a detector is processed to form a likelihood ratio; as successive samples are collected, the evolution of the likelihood ratio is equivalent to a discrete-time biased random walk [2]. In continuous-time implementations of sequential binary hypothesis tests, evidence accumulation is represented through diffusive stochastic differential equations [3]. The relationship between discrete and continuous implementations of the SPRT is discussed in [2], where it is shown how the logarithmic likelihood ratio in the SPRT converges in distribution to a stochastic differential equation with constant drift and diffusion terms: the *drift-diffusion model (DDM)*. The DDM is also used to study cognitive and neural processes underlying decisions in humans and animals [2].

We adopt the DDM as a basis for modeling information accumulation by a single unit, and we study networks of DDMs in which communication of information among the units occurs according to the Laplacian flow [4]. Similar models of communication have been used in the study of collective decision making in social networks as well as in distributed implementations of hypothesis testing problems in the engineering literature [6]. In fact, our information aggregation model is the continuous-time equivalent of the running consensus algorithm with fixed network structure [6]. Such networks of DDMs have been applied in [7], [8] to analyze the performance of consensus protocols in the presence of noise as a function of effective resistance of the network graph. The notion of effective resistance is relevant to many fields beyond consensus; see [9], and [10] which also discussed the connection between error covariance and effective resistance in estimation.

Rather than analyzing the collective effect of noise—as is common in the consensus literature [7], [8]—this technical note focuses on assessing the contribution of each individual unit to the uncertainty of the network process. We consider a network of agents with drift-diffusion dynamics interconnected according to a general communication graph. An example of such a system is a network of unmanned aerial vehicles (UAVs), each equipped with a camera and/or other sensing modalities—e.g., heat or smoke detectors—to monitor a forested region for fire, and each communicating its evidence for the presence of fire to its neighbors according to a fixed graph.

Among all directed graphs satisfying a mild connectivity assumption, we prove that balanced digraphs are the ones that minimize the linear growth rate of the variance of each node. For this class of graphs, we introduce an index that characterizes the certainty of each unit, and we interpret this index in terms of a generalization of the notion of effective resistance to directed graphs [11]. Restricted to graphs with normal Laplacian matrices, which include all undirected graphs, our results formally relate node certainty to information centrality developed in [12] in the context of social networks. We prove that the ordering of nodes by certainty is determined by the ordering of nodes by information centrality. In the fire-detection example described

Manuscript received September 10, 2013; revised September 9, 2014 and March 28, 2015; accepted June 26, 2015. Date of publication July 8, 2015; date of current version March 25, 2016. This work was supported in part by AFOSR Grant FA9550-07-1-0-0528, ONR Grants N00014-09-1-1074, N00014-14-1-0635, NSF Grant ECCS-1135724, ARO Grants W911NG-11-1-0385 and W911NF-14-1-0431, and by NSERC. Recommended by Associate Editor C. Hadjicostis.

I. Poulakakis is with the Department of Mechanical Engineering, University of Delaware, Newark, DE 19711 USA (e-mail: poulakas@udel.edu).

G. F. Young and N. E. Leonard are with the Department of Mechanical and Aerospace Engineering, Princeton University, Princeton, NJ 08544 USA (e-mail: gfyoung@princeton.edu; naomi@princeton.edu).

L. Scardovi is with the Department of Electrical and Computer Engineering, University of Toronto, Toronto, ON M5S 3G4, Canada (e-mail: scardovi@scg.utoronto.ca).

Color versions of one or more of the figures in this paper are available online at http://ieeexplore.ieee.org.

Digital Object Identifier 10.1109/TAC.2015.2454373

above, these results imply that the more information central is a UAV in the communication graph, the more accurate is its assessment regarding the presence of fire. Then, a reliable detection strategy would have the most information central UAVs dominate the group's decision. Preliminary parts of this technical note appeared in [13], [14]; see also [26] for a more detailed account.

II. Model and Problem Statement

A. Networks of Sequential Evidence Accumulators

In the context of two-choice decisions—e.g, if there is a fire or not—the diffusive paradigm of evidence accumulation admits a simple representation [2]. Under the assumption that the difference between the amounts of evidence supporting each of the two choices is integrated over time, evidence is accumulated according to the drift-diffusion model (DDM)

$$dx = \beta dt + \sigma dW \tag{1}$$

where $x(t)$ is the accumulated value at time t of the difference in the information favoring one choice over the other, and $x = 0$ if the integrated evidences are equal. In (1), the constant drift β represents an increase in the evidence supporting the correct choice and σdW are increments drawn from a Wiener process with standard deviation σ. Equation (1) is the (weak) limit of the logarithmic likelihood ratio in typical binary hypothesis tests under the assumption that infinitesimal increments of information arrive at each moment in time [2].

We focus on a network of n evidence accumulating units as the interconnection of n DDMs that share the relative value of their evidence with those units with which they can communicate. The state x_k of unit k, for each $k = 1, \ldots, n$, evolves according to

$$dx_k = \left[\beta + \sum_{j=1}^{n} \alpha_{kj}(x_j - x_k)\right] dt + \sigma dW_k \tag{2}$$

where $\alpha_{kj} \geq 0$ denotes the attention paid by unit k to the difference between its state x_k and the state x_j of unit j; $\alpha_{kj} = 0$ implies that the units k and j do not communicate. The constant drift β and the independent Wiener processes σdW_k are the same as in (1).

The model (2) can be associated with a collective decision-making scenario, in which a set of interconnected decision-making units is presented with partial information about a stimulus—e.g., a deterministic signal corrupted by noise—and each unit is asked to identify it between two alternatives within a finite time interval [13]. More recently, (2) has been used to investigate the speed-accuracy tradeoff in collective implementations of two-alternative decision-making tasks in [15] and to consider the case in which a limited number of units can measure the external signal directly [16].

The model (2) with $\beta = 0$ has been used to determine necessary and sufficient conditions for mean-square average consensus under measurement noise [17], and to analyze the stochastic stability [8], and robustness [7], of linear consensus algorithms in the presence of (white) noise. Similar models have been employed in [18] to study whether local feedback is sufficient to maintain coherence in large-scale networks under the influence of stochastic disturbances and in [16], [19], [20] to find leaders that maximize robustness in stochastically forced consensus networks. A common metric for assessing the quality of consensus under measurement noise is the trace of the covariance matrix associated with the projection of the state on the subspace orthogonal to the consensus subspace [7], [8], [21]. Such metrics capture the *collective* effect of the uncertainty, but they do not distinguish the *individual* contributions of the nodes to the dispersion around the consensus subspace. Here, we address how the uncertainty of each node affects the total uncertainty of the process, and how a node's contribution can be characterized based on its location in the underlying interconnection graph.

B. Notation and Basic Properties of the Model

We identify the communication topology in the network with a digraph $\mathcal{G} = (\mathcal{V}, \mathcal{E}, A)$. The vertex set $\mathcal{V} := \{v_1, \ldots, v_n\}$ contains n nodes that represent the n evidence accumulators. The edge set $\mathcal{E} \subseteq \mathcal{V} \times \mathcal{V}$ contains the communication links among the nodes, and $A \in \mathbb{R}_{\geq 0}^{n \times n}$ is the corresponding weighted adjacency matrix. The elements of A are denoted by $\alpha_{kj} \geq 0$ such that $\alpha_{kj} > 0$ if $e_{kj} = (v_k, v_j) \in \mathcal{E}$, and $\alpha_{kj} = 0$ otherwise. We adopt a "sensing" convention: a (directed) edge $e_{kj} = (v_k, v_j) \in \mathcal{E}$ implies that node v_j transmits information about its state to node v_k; equivalently, v_k can "sense" the state of v_j, and we say v_j is a "neighbor" of v_k. We will assume that there are no self-loops in $\mathcal{G}$, i.e., $\alpha_{kk} = 0$ for all $v_k \in \mathcal{V}$. The out- and in-degree of a node $v_k \in \mathcal{V}$ can be defined, respectively, by $\deg_{\text{out}}(v_k) := \sum_{j=1}^{n} \alpha_{kj}$ and $\deg_{\text{in}}(v_k) := \sum_{j=1}^{n} \alpha_{jk}$. If $\deg_{\text{out}}(v_k) = \deg_{\text{in}}(v_k)$ for all $v_k \in \mathcal{V}$, graph $\mathcal{G}$ is *balanced*. In this notation, (2) becomes

$$dx = (b - Lx)dt + HdW \tag{3}$$

where $x := \text{col}(x_1, \ldots, x_n)$, $dW := \text{col}(dW_1, \ldots, dW_n)$, $b := \beta \mathbf{1}_n$ and $H := \sigma I_n$; $\mathbf{1}_n$ is the n-dimensional vector with entries all equal to one and I_n is the $n \times n$ identity matrix. In (3), L is the Laplacian matrix associated with $\mathcal{G}$, defined by $L_{kj} := \sum_{i=1, i \neq k}^{n} \alpha_{ki}$ for $k = j$ and $L_{kj} := -\alpha_{kj}$ for $k \neq j$. By construction, $\mathbf{1}_n$ is an eigenvector of L corresponding to the eigenvalue $\lambda_1 = 0$. We will use the Laplacian on the subspace of $\mathbb{R}^n$ orthogonal to $\mathbf{1}_n$. Consider an $(n-1) \times n$ matrix Q with rows that form an orthonormal basis for this subspace and that satisfies

$$Q\mathbf{1}_n = \mathbf{0}_{n-1}, \quad QQ^{\mathrm{T}} = I_{n-1} \text{ and } Q^{\mathrm{T}}Q = I_n - \frac{1}{n}\mathbf{1}_n\mathbf{1}_n^{\mathrm{T}}. \tag{4}$$

Then, the *reduced Laplacian* matrix is given by

$$L_r = QLQ^{\mathrm{T}}. \tag{5}$$

If the graph is balanced, $\mathbf{1}_n^{\mathrm{T}}$ is a left eigenvector of L with $\lambda_1 = 0$. A (directed) path in a digraph $\mathcal{G}$ is an ordered sequence of vertices, such that any pair appearing consecutively is an edge of the digraph, and every vertex other than the first and last is unique. A vertex of a digraph is *globally reachable* if, and only if, it can be reached from any other vertex by traversing a directed path. A digraph $\mathcal{G}$ is *strongly connected* if, and only if, every vertex is globally reachable. For balanced digraphs, containing a globally reachable node is equivalent to being strongly connected (and implies weaker notions of connectivity) [22]. Next, we summarize properties of L.

Proposition 1: Let $\mathcal{G} := (\mathcal{V}, \mathcal{E}, A)$ be a digraph of order n, and L its associated Laplacian. Then:

(i) all the eigenvalues of L have nonnegative real parts;
(ii) if $\mathcal{G}$ contains a globally reachable node, then $\text{rank}(L) = n - 1$, i.e., 0 is a simple eigenvalue of L;
(iii) for any $\tau \in [0, t]$, $e^{-L(t-\tau)}$ is a row-stochastic matrix.

Statements (i) and (ii) are proved in [23], and statement (iii) is a direct consequence of the fact that the rows of L sum to zero.

It is known from general results in [24, pp. 131–132] that the stochastic process $\{x(t) : t \geq 0\}$ produced by (3) is Gaussian. Moreover, assuming that $x(0) = 0$ with probability one, the mean and covariance of $x(t)$ are given, respectively, by

$$\mathbb{E}[x(t)] = \int_0^t e^{-L(t-\tau)} b d\tau \tag{6}$$

$$\text{Cov}(x(t), x(t)) = \sigma^2 \int_0^t e^{-L(t-\tau)} e^{-L^{\mathrm{T}}(t-\tau)} d\tau. \tag{7}$$

The lemma below provides lower and upper bounds for the variance of the state of each unit. The lower bound is used in Section III to define an index that characterizes the certainty of each unit.

Lemma 1: Consider (3). For any interconnection digraph $\mathcal{G} = (\mathcal{V}, \mathcal{E}, A)$ and any node $v_k \in \mathcal{V}$

$$\mathbb{E}\left[x_k(t)\right] = \beta t \tag{8}$$

$$\frac{\sigma^2}{n} t \leq \mathrm{Var}\left(x_k(t)\right) \leq \sigma^2 t. \tag{9}$$

Proof: Equation (8) follows from (6) for $b = \beta \mathbf{1}_n$, since, by Proposition 1(iii), $e^{-L(t-\tau)}$ is row-stochastic. To show (9), let $\mathbf{q}_k$ be the $n \times 1$ vector with all elements equal to zero except element k, which is equal to one; note that $\sum_{k=1}^{n} \mathbf{q}_k = \mathbf{1}_n$. Then

$$\begin{aligned}\mathrm{Var}\left(x_k(t)\right) &= \mathbf{q}_k^{\mathrm{T}} \mathrm{Cov}\left(x(t), x(t)\right) \mathbf{q}_k \\ &= \sigma^2 \int_0^t \left\| e^{-L^{\mathrm{T}}(t-\tau)} \mathbf{q}_k \right\|_2^2 d\tau\end{aligned}$$

where (7) has been used. The result now follows from $(1/n)\left\|e^{-L^{\mathrm{T}}(t-\tau)}\mathbf{q}_k\right\|_1^2 \leq \left\|e^{-L^{\mathrm{T}}(t-\tau)}\mathbf{q}_k\right\|_2^2 \leq \left\|e^{-L^{\mathrm{T}}(t-\tau)}\mathbf{q}_k\right\|_1^2$, where $\left\|e^{-L^{\mathrm{T}}(t-\tau)}\mathbf{q}_k\right\|_1 = 1$, since $e^{-L^{\mathrm{T}}(t-\tau)}\mathbf{q}_k$ is the k-th row of $e^{-L(t-\tau)}$, which is row-stochastic by Proposition 1(iii). ■

Remark 1: Lemma 1 shows that the expected value of the evidence accumulated by each unit increases linearly with time at a rate β, which is the same for all units regardless of the interconnection topology. By way of contrast, the covariance matrix does depend on the interconnection. This implies that certain communication topologies—and certain nodes within them—may be better than others in terms of certainty in integrating information. In view of the fact that $\sigma^2 t$ is the variance of the state of an isolated DDM, the upper bound in (9) implies that the uncertainty associated with any of the interconnected units cannot exceed that of an isolated unit.

Remark 2: When t is sufficiently small, by expanding the exponentials in (7) in Taylor series and neglecting higher order terms, $\mathrm{Cov}(x(t), x(t)) \approx (\sigma^2 t) I_n$. This implies that all units behave like isolated DDMs at the beginning of the process. It will become apparent in the following sections that, as time evolves and the units collect and communicate their accumulated evidence, their certainty improves with respect to that of an isolated DDM in a way that depends on the topology of the communication. We identify units with variance that evolves more closely to the lower bound in (9).

III. Balanced Graphs and Node Certainty

This section characterizes the class of digraphs in which node variance evolves within a bounded constant from the lower bound $\sigma^2 t/n$ established by Lemma 1. For this class, we introduce an index that encodes the certainty of each unit as it accrues evidence and can be used to rank the nodes according to the quality of their accumulated data. The next proposition establishes conditions under which the difference between the variance of the state of each node and the minimum possible variance $\sigma^2 t/n$ remains bounded.

Proposition 2: Let $\mathcal{G} := (\mathcal{V}, \mathcal{E}, A)$ be a digraph, and L its associated Laplacian. Assume that $\mathcal{G}$ contains a globally reachable node. Then, after initial transients:

(i) the variance of each node increases linearly with time;
(ii) the linear growth rate of the variance of every $v_k \in \mathcal{V}$ is σ^2/n if, and only if, $\mathcal{G}$ is balanced;
(iii) if $\mathcal{G}$ is not balanced, the variance of every node will have growth rate strictly larger than σ^2/n.

To prove Proposition 2, we will use the following lemma regarding the structure of the covariance matrix (7).

Lemma 2: Consider (3). Under the conditions and notation of Proposition 2, the covariance matrix (7) takes the form

$$\mathrm{Cov}\left(x(t), x(t)\right) = \sigma^2 \left(C_0 + C_1 t + C_2(t)\right) \tag{10}$$

where $C_0 = -SL_r^{-2T}QL^{\mathrm{T}} - LQ^{\mathrm{T}}L_r^{-2}S^{\mathrm{T}}$, $C_1 = (1/n)\mathbf{1}_n\mathbf{1}_n^{\mathrm{T}} + SS^{\mathrm{T}}$, $C_2(t) = S\mathrm{e}^{-L_r^{\mathrm{T}}t}L_r^{-\mathrm{T}}QL^{\mathrm{T}} + LQ^{\mathrm{T}}L_r^{-1}\mathrm{e}^{-L_r t}S^{\mathrm{T}} + LQ^{\mathrm{T}}L_r^{-1}\Sigma(t)L_r^{-\mathrm{T}}QL^{\mathrm{T}}$ with $S := LQ^{\mathrm{T}}L_r^{-1} - Q^{\mathrm{T}}$, and

$$\Sigma(t) := \int_0^t \mathrm{e}^{-L_r(t-\tau)}\mathrm{e}^{-L_r^{\mathrm{T}}(t-\tau)}\, d\tau \tag{11}$$

in which Q is a matrix defined as in (4) and L_r is the corresponding reduced Laplacian given by (5).

Proof: Let $P = \left[(1/\sqrt{n})\mathbf{1}_n \;\; Q^{\mathrm{T}}\right]^{\mathrm{T}}$ where Q satisfies (4); clearly, P is orthogonal. Next, note that

$$PLP^{\mathrm{T}} = \begin{bmatrix} 0 & \frac{1}{\sqrt{n}}\mathbf{1}_n^{\mathrm{T}}LQ^{\mathrm{T}} \\ \mathbf{0}_{n-1} & L_r \end{bmatrix} \tag{12}$$

$$P\mathrm{e}^{Lt}P^{\mathrm{T}} = \begin{bmatrix} 1 & \frac{1}{\sqrt{n}}\mathbf{1}_n^{\mathrm{T}}LQ^{\mathrm{T}}L_r^{-1}\left(\mathrm{e}^{L_r t} - I_{n-1}\right) \\ \mathbf{0}_{n-1} & \mathrm{e}^{L_r t} \end{bmatrix} \tag{13}$$

which follow from properties of P and L. Re-writing (7) as

$$\mathrm{Cov}(x(t), x(t)) = \sigma^2 P^{\mathrm{T}} \int_0^t P\mathrm{e}^{-L(t-\tau)}P^{\mathrm{T}}P\mathrm{e}^{-L^{\mathrm{T}}(t-\tau)}P^{\mathrm{T}}d\tau P$$

and substituting (12), (13) and their transposes results in (10). ■

With the aid of Lemma 2, we can prove Proposition 2.

Proof [Proposition 2]: The assumption that $\mathcal{G}$ contains a globally reachable node implies that $-L_r$ is Hurwitz [7, Lemma 1]. Hence, $\lim_{t\to\infty}\mathrm{e}^{-L_r t} = \lim_{t\to\infty}\mathrm{e}^{-L_r^{\mathrm{T}}t} = 0$ and $\lim_{t\to\infty}\Sigma(t) = \Sigma$, the unique positive-definite matrix that satisfies Lyapunov's equation

$$L_r\Sigma + \Sigma L_r^{\mathrm{T}} = I_{n-1} \tag{14}$$

see also [7, Lemma 2]. As a result

$$\lim_{t\to\infty} C_2(t) = LQ^{\mathrm{T}}L_r^{-1}\Sigma L_r^{-\mathrm{T}}QL^{\mathrm{T}} =: C_{2,\mathrm{ss}}$$

a constant matrix. Hence, after initial transients, the variance associated with $v_k \in \mathcal{V}$ converges to

$$\mathrm{Var}\left(x_k(t)\right) \to \sigma^2\left(\mathbf{q}_k^{\mathrm{T}}(C_0 + C_{2,\mathrm{ss}})\mathbf{q}_k + \left(\mathbf{q}_k^{\mathrm{T}}C_1\mathbf{q}_k\right)t\right) \tag{15}$$

confirming (i). To show (ii) and (iii), we focus on the linear term $\sigma^2(\mathbf{q}_k^{\mathrm{T}}C_1\mathbf{q}_k)t$ in (15), which by Lemma 2 becomes

$$\sigma^2\left(\frac{1}{n} + \mathbf{q}_k^{\mathrm{T}}SS^{\mathrm{T}}\mathbf{q}_k\right)\, t = \sigma^2\left(\frac{1}{n} + \left\|S^{\mathrm{T}}\mathbf{q}_k\right\|_2^2\right)\, t.$$

Using the fact that $S = LQ^{\mathrm{T}}L_r^{-1} - Q^{\mathrm{T}} = (1/n)\mathbf{1}_n\mathbf{1}_n^{\mathrm{T}}LQ^{\mathrm{T}}L_r^{-1}$, which follows directly from the properties (4) of Q, we deduce that the term $\left\|S^{\mathrm{T}}\mathbf{q}_k\right\|_2^2$ is equal to zero when $S^{\mathrm{T}}\mathbf{q}_k = \mathbf{0} \Leftrightarrow QL^{\mathrm{T}}\mathbf{1}_n = \mathbf{0} \Leftrightarrow L^{\mathrm{T}}\mathbf{1}_n = \mathbf{0}$, i.e., for balanced $\mathcal{G}$. When $\mathcal{G}$ is not balanced, the linear growth rate of the variance of any node will be strictly greater than σ^2/n. ■

Motivated by Proposition 2, we restrict our analysis to strongly connected digraphs $\mathcal{G} = (\mathcal{V}, \mathcal{E}, A)$ that are balanced. In these graphs, and for each $v_k \in \mathcal{V}$ we can define the *node certainty index* $\mu : \mathcal{V} \to \mathbb{R}_{>0} \cup \{\infty\}$ as the inverse of the difference between the variance $\mathrm{Var}(x_k(t))$ of the state x_k of node v_k and the minimum possible variance $\sigma^2 t/n$ as $t \to +\infty$; that is

$$\frac{1}{\mu(v_k)} := \lim_{t\to+\infty}\left(\mathrm{Var}\left(x_k(t)\right) - \sigma^2\frac{t}{n}\right). \tag{16}$$

A high value of $\mu(v_k)$ corresponds to small uncertainty associated with the node v_k, since the variance of its state evolves closely to the minimum possible variance $\sigma^2 t/n$; see Lemma 1. By convention, $\mu(v_k) = \infty$ corresponds to the highest possible certainty. Classifying the nodes of a graph based on their certainty index and interpreting this classification in terms of the structural properties of the interconnection graph will be discussed in Section IV below. First, we state a proposition that shows μ is well defined for strongly connected balanced digraphs and provides a formula for computing μ.

Proposition 3: Let $\mathcal{G} := (\mathcal{V}, \mathcal{E}, A)$ be a digraph, and L its Laplacian. Assume that $\mathcal{G}$ is strongly connected and balanced. Then:

(i) the limit in (16) is finite;
(ii) with the notation above, the index μ is computed by

$$\frac{1}{\mu(v_k)} = \sigma^2 \, \mathbf{q}_k^{\mathrm{T}} (Q^{\mathrm{T}} \Sigma Q) \mathbf{q}_k. \tag{17}$$

The proof of Proposition 3 is a straightforward consequence of Lemma 2 and Proposition 2 and will be omitted. To provide further intuition on the node certainty index μ, Corollary 1 particularizes Proposition 3 to strongly connected digraphs $\mathcal{G} = (\mathcal{V}, \mathcal{E}, A)$ with Laplacian matrices L that are normal; i.e., matrices that commute with their transpose, [25, Sec. 2.5]. This family of graphs includes all the undirected graphs, and also some classes of directed graphs, such as directed circulant graphs; see [26, Section V] for more details.

Corollary 1: In addition to the conditions of Proposition 3, assume that the corresponding Laplacian L is normal. Then, for $v_k \in \mathcal{V}$ the node certainty index μ can be computed by

$$\frac{1}{\mu(v_k)} = \sigma^2 \sum_{p=2}^{n} \frac{1}{2\mathrm{Re}(\lambda_p)} \left| u_k^{(p)} \right|^2 \tag{18}$$

where $\mathrm{Re}(\lambda_p)$ is the real part of the eigenvalue λ_p, $p \in \{2, \ldots, n\}$ of L, and $u_k^{(p)}$ is the k-th component of the p-th normalized eigenvector.

Proof: By [25, Theorem 2.5.4], the normality of L implies that there exists a unitary matrix U such that $U^* L U = \Lambda$, where U^* is the Hermitian transpose of U and Λ is a diagonal matrix with the eigenvalues of L. Partition U as $U = [u^{(1)} | \ldots | u^{(n)}] = [u^{(1)} \mid U_r]$, where $u^{(1)} = (1/\sqrt{n})\mathbf{1}_n$ and U_r contains the normalized eigenvectors $u^{(p)}$ corresponding to the nonzero eigenvalues $\lambda_p, p = 2, \ldots, n$. Then, (5) becomes $L_r = Q U_r \Lambda_r U_r^* Q^{\mathrm{T}}$, where Λ_r is the diagonal matrix containing the nonzero eigenvalues of L. Hence, (11) gives

$$\Sigma = Q U_r \left(\int_0^{\infty} e^{-(\Lambda_r + \bar{\Lambda}_r)(t-\tau)} d\tau \right) U_r^* Q^{\mathrm{T}} \tag{19}$$

where $\bar{\Lambda}_r$ is the complex conjugate of Λ_r. The result follows from (17) through pre- and post-multiplying (19) by Q^{T} and Q, respectively, and using (4) and the facts $\mathbf{1}_n^{\mathrm{T}} U_r = U_r^* \mathbf{1}_n = 0$. ■

The additional structure imposed on the Laplacian L by requiring it to be a normal matrix renders the dependence of the node certainty index μ on the eigenstructure of L explicit, as shown by (17). This allows us to draw connections between μ and the total effective resistance, or the Kirchhoff index, K_{f}, of the underlying graph.

Remark 3: Under the conditions of Corollary 1, (18) results in

$$\sum_{v_k \in \mathcal{V}(\mathcal{G})} \frac{1}{\mu(v_k)} = \sigma^2 \sum_{p=2}^{n} \frac{1}{2\mathrm{Re}(\lambda_p)}. \tag{20}$$

For linear consensus protocols in the presence of additive white noise, the sum on the right hand side of (20) corresponds to the expected steady-state dispersion around the consensus subspace. Hence, the inverse of $\mu(v_k)$ can be interpreted as the *individual* contribution of the node v_k to the dispersion of the evidence; the higher $\mu(v_k)$, the smaller the contribution of the node v_k. In the case of undirected graphs, the sum (20) is related to the total effective resistance K_{f}, or Kirchhoff index, $K_{\mathrm{f}} = n \sum_{p=2}^{n} (1/\lambda_p)$ of the graph; see [9]. So, for undirected graphs, we have $\sum_{v_k \in \mathcal{V}(\mathcal{G})} (1/\mu(v_k)) = \sigma^2 (K_{\mathrm{f}}/2n)$.

IV. Node Certainty as a Centrality Measure

In this section, the node certainty index μ is characterized in terms of the structural properties of the underlying interconnection graph and shown to depend on the *totality* of paths in the network.

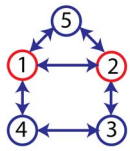

Vertex	Degree	κ_{close}	μ
v_1	3	1.00	8.33
v_2	3	1.00	8.33
v_3	2	0.83	5.26
v_4	2	0.83	5.26
v_5	2	0.83	5.00

Fig. 1. Left: The connected undirected graph used to illustrate that *all* paths—not just the geodesics—must be taken into account in interpreting μ. The nodes that maximize the certainty index are v_1 and v_2, and the node that minimizes certainty is v_5. Right: Node properties (degree, κ_{close} and μ).

A. A Motivational Example

Consider the undirected graph in Fig. 1 [12]. For each node v_k, we compute the certainty index $\mu(v_k)$ using (17), and its degree, i.e., the number of edges attached to v_k. The corresponding *closeness* centrality, κ_{close}, is provided as a representative geodesic-distance-based measure of centrality. Defining the geodesic distance $d(v_k, v_j)$ between v_k and v_j as the length of the *shortest* path connecting them, the closeness centrality of a node v_k is computed as the inverse of the mean geodesic distance $d(v_k, v_j)$ over all nodes v_j

$$\kappa_{\mathrm{close}}(v_k) = \left(\frac{1}{n} \sum_{j=1}^{n} d(v_k, v_j) \right)^{-1} \tag{21}$$

see [27, Section 7.6]. The example of the graph of Fig. 1 demonstrates that, for general undirected graphs, node certainty cannot be captured by centrality measures based on degrees or geodesic paths. This is a consequence of the fact that the evidence accumulated by each unit is transmitted through the network and reaches the rest of the units via circuitous, non-geodesic pathways.

As an example, note that $\mu(v_3) = \mu(v_4) > \mu(v_5)$ in Fig. 1. This distinction between v_5 and $\{v_3, v_4\}$ cannot be captured by their degrees, which are all equal to 2, nor by their closeness centralities, which are all equal to 0.83, nor by *any* centrality measure that is defined based on geodesic paths. To see this, note that any of the vertices v_3, v_4, and v_5 in the graph of Fig. 1 is connected to the rest through two geodesic paths of length 2 and two geodesic paths of length 1. Hence, excluding non-geodesic pathways, these nodes are equivalent, resulting in $\kappa_{\mathrm{close}}(v_3) = \kappa_{\mathrm{close}}(v_4) = \kappa_{\mathrm{close}}(v_5)$.

B. Main Result: Node Certainty and Information Centrality

This section clarifies the relation between node certainty, as characterized by the index μ, and the location of a node in the underlying interconnection graph through the notion of effective resistance.

We begin with defining effective resistance for strongly connected weighted balanced digraphs. Let $\mathcal{G} = (\mathcal{V}, \mathcal{E}, A)$ be such a digraph. Following [11], we can compute effective resistances between any pair of nodes in $\mathcal{G}$ from the corresponding Laplacian matrix L as follows. Let $v_k, v_j \in \mathcal{V}$ be two nodes with $v_k \neq v_j$. Then, the *directed effective resistance* between v_k and v_j is given by

$$r(v_k, v_j) = x_{kk} + x_{jj} - 2x_{kj} \tag{22}$$

where x_{kj}, $1 \leq k, j \leq n$ are the entries of the matrix

$$X := 2Q^{\mathrm{T}} \Sigma Q \tag{23}$$

and Q is defined through (4) and Σ is the solution of (14) with L_r the reduced Laplacian computed by (5). Finally, we can compute the total effective resistance of $\mathcal{G}$ as

$$K_{\mathrm{f}} = \sum_{k<j} r(v_k, v_j) \tag{24}$$

which generalizes the Kirchhoff index defined for undirected graphs to strongly connected balanced digraphs.

We now define the *directed information centrality* of v_k as the inverse of the mean effective resistance $r(v_k, v_j)$ over all nodes v_j

$$\kappa_{\text{info}}(v_k) := \left(\frac{1}{n} \sum_{j=1}^{n} r(v_k, v_j) \right)^{-1}. \tag{25}$$

Our motivation for using the term information centrality in (25) comes from the work of Stephenson and Zelen [12] on social networks. It will be shown below that (25) essentially represents a generalization of the original definition of information centrality in [12] to balanced digraphs that are strongly connected. Note the similarities between (21) and (25), with the important difference being that κ_{info} depends on all connections between nodes.

Theorem 1 below relates the certainty index of a node v_k in a balanced and strongly connected weighted digraph $\mathcal{G} = (\mathcal{V}, \mathcal{E}, A)$ to the directed information centrality of v_k.

Theorem 1: Let $\mathcal{G} = (\mathcal{V}, \mathcal{E}, A)$ be a balanced and strongly connected digraph on n vertices. Then, the certainty index $\mu(v_k)$ of the node $v_k \in \mathcal{V}$ is

$$\frac{1}{\mu(v_k)} = \frac{\sigma^2}{2} \left(\frac{1}{\kappa_{\text{info}}(v_k)} - \frac{K_{\text{f}}}{n^2} \right)$$

where $\kappa_{\text{info}}(v_k)$ is the information centrality of v_k in $\mathcal{G}$ and K_{f} is the Kirchhoff index of $\mathcal{G}$ given by (24). Hence, for any set of indices $k_1, k_2, \ldots, k_n$, the following inequalities are equivalent:

$$\mu(v_{k_1}) \geq \mu(v_{k_2}) \geq \cdots \geq \mu(v_{k_n})$$
$$\kappa_{\text{info}}(v_{k_1}) \geq \kappa_{\text{info}}(v_{k_2}) \geq \cdots \geq \kappa_{\text{info}}(v_{k_n}).$$

Theorem 1 shows that node ranking according to certainty is determined by the graph structure via the notion of effective resistance. In particular, more certain nodes are located so that they minimize the mean effective resistance averaged over all nodes of the graph. To provide more intuition, we consider the special case of strongly-connected weighted digraphs with normal Laplacian matrices. By Corollary 2 below, node ranking in this class of directed graphs is captured by their corresponding mirror graphs, which are undirected. To define the mirror graph $\hat{\mathcal{G}}$ of a strongly-connected normal digraph $\mathcal{G} = (\mathcal{V}, \mathcal{E}, A)$, let $\tilde{\mathcal{E}}$ be the set of reverse edges of $\mathcal{G}$, obtained by reversing the order of nodes of all pairs in $\mathcal{E}$. Then, $\hat{\mathcal{G}}$ is an undirected graph $\hat{\mathcal{G}} = (\hat{\mathcal{V}}, \hat{\mathcal{E}}, \hat{A})$ with set of vertices $\hat{\mathcal{V}} = \mathcal{V}$, set of edges $\hat{\mathcal{E}} := \mathcal{E} \cup \tilde{\mathcal{E}}$, and adjacency matrix $\hat{A} = [\hat{\alpha}_{kj}]$ with $\hat{\alpha}_{kj} = \hat{\alpha}_{jk} = (\alpha_{kj} + \alpha_{jk})/2$; see also [4, Def. 2].

Since $\hat{\mathcal{G}} = (\hat{\mathcal{V}}, \hat{\mathcal{E}}, \hat{A})$ is undirected and connected we can define information centrality in a more intuitive way, using a path enumeration procedure. Assume that $w : \hat{\mathcal{E}} \to \mathbb{R}_{>0}$ is a function that maps each edge $e \in \hat{\mathcal{E}}$ to its positive weight and consider a pair of vertices v_k, $v_j \in \hat{\mathcal{V}}$. Suppose there are m_{kj} paths $\mathcal{P}_{kj}(r)$, $r = 1, \ldots, m_{kj}$, connecting v_k and v_j and define the *weighted length* of $\mathcal{P}_{kj}(r)$ as

$$\ell_w(\mathcal{P}_{kj}(r)) := \sum_{e \in \mathcal{P}_{kj}(r)} \frac{1}{w(e)}. \tag{26}$$

The definition of the length ℓ_w in (26) reflects the convention that the higher the weight of an edge the more important the communication between the incident nodes of that edge is; hence, these nodes appear to be "closer." Additionally, the weighted length of a path matches the usual notion of effective resistance for undirected graphs [9].

To capture non-geodesic paths, we define the distance between v_k and v_j based on a "combined" path $\tilde{\mathcal{P}}_{kj}$ that incorporates all the paths $\mathcal{P}_{kj}(r)$, $r = 1, \ldots, m_{kj}$, connecting v_k and v_j. To do so, define the $m_{kj} \times m_{kj}$ matrix D_{kj} as follows: its diagonal entries $D_{kj}(r, r)$ correspond to the weighted lengths of the paths $\mathcal{P}_{kj}(r)$, $D_{kj}(r, r) = \ell_w(\mathcal{P}_{kj}(r))$, and its off-diagonal entries $D_{kj}(r, s)$ correspond to the sum of the inverse weights of the edges that are common between $\mathcal{P}_{kj}(r)$ and $\mathcal{P}_{kj}(s)$ for $r, s \in \{1, \ldots, m_{kj}\}$ with $r \neq s$, i.e., $D_{kj}(r, s) = \sum_{e \in \mathcal{P}_{kj}(r) \cap \mathcal{P}_{kj}(s)} (1/w(e))$. Then, the length $\ell_w(\tilde{\mathcal{P}}_{kj})$ of the combined path is given by

$$\frac{1}{\ell_w(\tilde{\mathcal{P}}_{kj})} = \sum_{r=1}^{m_{kj}} \sum_{s=1}^{m_{kj}} D_{kj}^{-1}(r, s) \tag{27}$$

and the distance between v_k and v_j is $\tilde{d}(v_k, v_j) := \ell_w(\tilde{\mathcal{P}}_{kj})$.

This procedure is analogous to combining resistances in parallel in electric circuits, while taking into account shared edges, so that the combined distance between two nodes is equal to the resistance distance between them; see Lemma 5 in Section IV-C .

Stephenson and Zelen in [12] define the total "information" contained in the entirety of paths connecting v_k and v_j as the inverse of the length of the combined path $I_{kj} := 1/\ell_w(\tilde{\mathcal{P}}_{kj})$, with $\ell_w(\tilde{\mathcal{P}}_{kj})$ computed by (27), and use I_{kj} to compute information centrality of a node v_k as the harmonic average

$$\hat{\kappa}_{\text{info}}(v_k) := \left(\frac{1}{n} \sum_{j=1}^{n} \frac{1}{I_{kj}} \right)^{-1} = \left(\frac{1}{n} \sum_{j=1}^{n} \tilde{d}(v_k, v_j) \right)^{-1}.$$

This corresponds to the restriction of (25) to the class of undirected weighted graphs.

With this notation, the following result can be stated.

Corollary 2: Let $\mathcal{G} = (\mathcal{V}, \mathcal{E}, A)$ be a strongly connected digraph on n vertices and assume that its Laplacian matrix L is normal. Then, the certainty index of the node $v_k \in \mathcal{V}$ is

$$\frac{1}{\mu(v_k)} = \frac{\sigma^2}{2} \left(\frac{1}{\hat{\kappa}_{\text{info}}(v_k)} - \frac{\hat{K}_{\text{f}}}{n^2} \right)$$

where $\hat{\kappa}_{\text{info}}(v_k)$ is the information centrality of v_k in the mirror graph $\hat{\mathcal{G}}$ of $\mathcal{G}$ and $\hat{K}_{\text{f}}$ is the Kirchhoff index of $\hat{\mathcal{G}}$ given by (24).

C. Proof of Main Result

In this section, Theorem 1 and Corollary 2 are proved through a sequence of lemmas. Theorem 1 follows from an examination of the covariance matrix given in (7).

Proof [Theorem 1]: Using (17) in view of (23) results in

$$\frac{1}{\mu(v_k)} = \frac{\sigma^2}{2} x_{kk}. \tag{28}$$

Then, from (25) and (22), we can write $\kappa_{\text{info}}(v_k) = (x_{kk} + (1/n)\text{Tr}(X))^{-1}$, since $X\mathbf{1}_n = 2Q^{\text{T}}\Sigma Q\mathbf{1}_n = \mathbf{0}_n$ by (4). Also because X is symmetric with zero row sums we have $K_{\text{f}} = n\text{Tr}(X)$. The result follows by substituting these expressions to (28). ■

To connect our algebraic notion of information centrality with the more intuitive, path-enumeration construction for undirected graphs, we start with a lemma due to Stephenson and Zelen [12].

Lemma 3 (Stephenson and Zelen, [12]): Let $\hat{\mathcal{G}} = (\hat{\mathcal{V}}, \hat{\mathcal{E}}, \hat{A})$ be an undirected connected graph of order n and let $\hat{L}$ be its Laplacian. Then, the total information I_{kj} transmitted via all paths connecting v_k, $v_j \in \hat{\mathcal{V}}$ is

$$I_{kj} = (c_{kk} + c_{jj} - 2c_{kj})^{-1} \tag{29}$$

where c_{kj}, $1 \leq k, j \leq n$, are the entries of $C = (\hat{L} + \mathbf{1}_n\mathbf{1}_n^{\text{T}})^{-1}$.

Next, we can derive an explicit formula for the matrix X from (23) for undirected graphs.

Lemma 4: Let $\hat{\mathcal{G}}$ be an undirected connected graph of order n with Laplacian matrix $\hat{L}$. Then, $\hat{X} = Q^{\text{T}}(Q\hat{L}Q^{\text{T}})^{-1}Q$, where $\hat{X}$ satisfies (23) for $\hat{\mathcal{G}}$.

Proof: Since $\hat{\mathcal{G}}$ is undirected, $\hat{L}$ is symmetric, and hence so is $\hat{L}_r = Q\hat{L}Q^{\mathrm{T}}$. Thus, (14) becomes $\hat{L}_r\hat{\Sigma} + \hat{\Sigma}\hat{L}_r = I$ which has solution $\hat{\Sigma} = (1/2)\hat{L}_r^{-1}$. The result follows by substituting $\hat{\Sigma}$ into (23). Note that $\hat{L}_r^{-1}$ exists since $\hat{\mathcal{G}}$ is connected, [7]. ■

The following lemma establishes a correspondence in undirected graphs between effective resistances $r(v_i, v_j)$, computed via (22), and the information I_{ij}, computed via (29).

Lemma 5: Let $\hat{\mathcal{G}}$ be an undirected connected graph of order n with Laplacian matrix $\hat{L}$. Then

$$C = \left(\hat{L} + \mathbf{1}_n\mathbf{1}_n^{\mathrm{T}}\right)^{-1} = \hat{X} + \frac{1}{n^2}\mathbf{1}_n\mathbf{1}_n^{\mathrm{T}} \tag{30}$$

where $\hat{X}$ is computed from $\hat{L}$ using (5), (14) and (23). Thus $r(v_i, v_j) = I_{i,j}^{-1}$ for all pairs of nodes (v_i, v_j) in $\hat{\mathcal{G}}$.

Proof: First, note that $\hat{L}$ is symmetric since $\hat{\mathcal{G}}$ is undirected, and $\hat{L}\mathbf{1}_n = \mathbf{0}_n$. Hence, we must have $\mathbf{1}_n^{\mathrm{T}}\hat{L} = \mathbf{0}_n^{\mathrm{T}}$ and hence $Q^{\mathrm{T}}Q\hat{L} = (I_n - (1/n)\mathbf{1}_n\mathbf{1}_n^{\mathrm{T}})\hat{L} = \hat{L}$. Then by Lemma 4, (30) follows from

$$\left(\hat{L} + \mathbf{1}_n\mathbf{1}_n^{\mathrm{T}}\right)\left(\hat{X} + \frac{1}{n^2}\mathbf{1}_n\mathbf{1}_n^{\mathrm{T}}\right) = Q^{\mathrm{T}}Q + \frac{1}{n}\mathbf{1}_n\mathbf{1}_n^{\mathrm{T}} = I_n$$

where (4) and $\mathbf{1}_n^{\mathrm{T}}\mathbf{1}_n = n$ have been used. By (30) we observe that $c_{ij} = \hat{x}_{ij} + (1/n^2)$, and the result follows from (29) and (22). ■

We now establish sufficient conditions for the computation of information centrality in digraphs using only the mirror graph.

Lemma 6: Let $\mathcal{G}$ be a strongly connected digraph on n vertices and assume that its Laplacian L is normal. Then, the information centrality $\kappa_{\mathrm{info}}(v_k)$ of node v_k in $\mathcal{G}$ is equal to the information centrality $\hat{\kappa}_{\mathrm{info}}(v_k)$ of node v_k in the mirror graph $\hat{\mathcal{G}}$ of $\mathcal{G}$.

Proof: By [7, Lemma 4], strongly connected digraphs with normal Laplacians are balanced. Then [4, Theorem 7] states that if $\mathcal{G}$ is balanced, the symmetric part $\hat{L} = (1/2)(L + L^{\mathrm{T}})$ of its Laplacian L is a valid Laplacian matrix for the mirror graph $\hat{\mathcal{G}}$ of $\mathcal{G}$. Now, by the proof of Lemma 4, we know that $\hat{\Sigma} = (1/2)\hat{L}_r^{-1}$ solves (14) for $\hat{\mathcal{G}}$. We will now show that $\hat{\Sigma}$ also solves (14) for $\mathcal{G}$.

First, $\hat{L}_r = (1/2)Q(L + L^{\mathrm{T}})Q^{\mathrm{T}} = (1/2)(L_r + L_r^{\mathrm{T}})$, implies that

$$\hat{\Sigma} = \left(L_r + L_r^{\mathrm{T}}\right)^{-1}. \tag{31}$$

Next, note that (4) results in $LQ^{\mathrm{T}}Q = L$ using the fact that $L\mathbf{1}_n = \mathbf{0}_n$. Furthermore, as $\mathcal{G}$ is balanced we also have $\mathbf{1}_n^{\mathrm{T}}L = \mathbf{0}_n^{\mathrm{T}}$, and hence $Q^{\mathrm{T}}QL = L$. Combining these expressions with the normality of L, i.e., $LL^{\mathrm{T}} = L^{\mathrm{T}}L$, results in

$$L_rL_r^{\mathrm{T}} = L_r^{\mathrm{T}}L_r \Rightarrow L_r^{-\mathrm{T}}L_r = L_rL_r^{-\mathrm{T}} \tag{32}$$

where we used the fact that L_r is invertible since $\mathcal{G}$ is connected; see [7, Lemma 1]. Equation (32) implies L_r is also normal.

To show that $\hat{\Sigma}$ also solves (14) for $\mathcal{G}$, we consider the term $L_r\hat{\Sigma} + \hat{\Sigma}L_r^{\mathrm{T}}$, which based on (31) and the results above gives

$$L_r\hat{\Sigma} + \hat{\Sigma}L_r^{\mathrm{T}} = I_{n-1} - \left(I_{n-1} + L_rL_r^{-\mathrm{T}}\right)^{-1} + \left(I_{n-1} + L_r^{-\mathrm{T}}L_r\right)^{-1}$$

where the Matrix Inversion Lemma was used. But by (32), the final two terms are identical with opposite signs. Hence, $\hat{\Sigma}$ solves (14) for $\mathcal{G}$ as well as $\hat{\mathcal{G}}$ implying that $X = \hat{X}$. The result follows. ■

Finally, Corollary 2 follows from Lemma 6 and Theorem 1.

V. Conclusion

This technical note proved that node certainty in a network of stochastic evidence accumulators depends on the underlying communication graph in a way that is captured by the notion of information centrality [12]. In recent work, this connection between information centrality and node certainty has been used to derive systematic solutions to the optimal leader selection problem for coherence in noisy networks [16], and to rigorously compare nodes in terms of their speed-accuracy tradeoffs in collective decision-making tasks [15]. Future work includes the generalization of these results to heterogeneous networks with different drifts and noise intensities among nodes.

References

[1] A. Wald, "Sequential tests of statistical hypotheses," *Ann. Math. Stat.*, vol. 16, no. 2, pp. 117–186, 1945.

[2] R. Bogacz, E. Brown, J. Moehlis, P. Holmes, and J. D. Cohen, "The physics of optimal decision making: A formal analysis of models of performance in two-alternative forced-choice tasks," *Psych. Rev.*, vol. 113, no. 4, pp. 700–765, 2006.

[3] J. Baras and A. LaVigna, "Real-time sequential detection for diffusion signals," in *Proc. IEEE Conf. Decision Control*, 1987, pp. 1153–1157.

[4] R. Olfati-Saber and R. Murray, "Consensus problems in networks of agents with switching topology and time-delays," *IEEE Trans. Autom. Control*, vol. 49, no. 9, pp. 1520–1533, Sep. 2004.

[5] M. O. Jackson, *Social and Economic Networks*. Princeton, NJ: Princeton Univ. Press, 2010.

[6] P. Braca, V. Marano, and V. Matta, "Enforcing consensus while monitoring the environment in wireless sensor networks," *IEEE Trans. Signal Process.*, vol. 76, no. 7, pp. 3375–3380, Jul. 2008.

[7] G. F. Young, L. Scardovi, and N. E. Leonard, "Robustness of noisy consensus dynamics with directed communication," in *Proc. Amer. Control Conf.*, 2010, pp. 6312–6317.

[8] G. S. Medvedev, "Stochastic stability of continuous time consensus protocols," *SIAM J. Control Optimiz.*, vol. 50, no. 4, pp. 1859–1885, 2012.

[9] A. Ghosh, S. Boyd, and A. Saberi, "Minimizing effective resistance of a graph," *SIAM Rev.*, vol. 50, no. 1, pp. 37–66, 2008.

[10] P. Barooah and J. P. Hespanha, "Estimation on graphs from relative measurements," *IEEE Control Syst. Mag.*, vol. 27, no. 4, pp. 57–74, Apr. 2007.

[11] G. F. Young, L. Scardovi, and N. E. Leonard, "A new notion of effective resistance for directed graphs—Part I: Definition and properties," arXiv:1310.5163, 2013.

[12] K. Stephenson and M. Zelen, "Rethinking centrality: Methods and examples," *Social Netw.*, vol. 11, no. 1, pp. 1–37, 1989.

[13] I. Poulakakis, L. Scardovi, and N. E. Leonard, "Coupled stochastic differential equations and collective decision making in the two-alternative forced-choice task," in *Proc. Amer. Contr. Conf.*, 2010, pp. 69–74.

[14] I. Poulakakis, L. Scardovi, and N. E. Leonard, "Node certainty in collective decision making," in *Proc. IEEE Conf. Decision Control*, 2012, pp. 4648–4653.

[15] V. Srivastava and N. E. Leonard, "Collective decision-making in ideal networks: The speed-accuracy tradeoff," *IEEE Trans. Control Netw. Syst.*, vol. 1, no. 1, pp. 121–130, Mar. 2014.

[16] K. Fitch and N. E. Leonard, "Information centrality and optimal leader selection in noisy networks," in *Proc. IEEE Conf. Decision Control*, 2013, pp. 7510–7515.

[17] T. Li and J.-F. Zhang, "Mean square average-consensus under measurement noises and fixed topologies: Necessary and sufficient conditions," *Automatica*, vol. 45, no. 8, pp. 1929–1936, 2009.

[18] B. Bamieh, M. R. Jovanović, P. Mitra, and S. Patterson, "Coherence in large-scale networks: Dimension-dependent limitations of local feedback," *IEEE Trans. Autom. Control*, vol. 57, no. 9, pp. 2235–2249, Sep. 2012.

[19] A. Clark, L. Bushnell, and R. Poovendran, "A supermodular optimization framework for leader selection under link noise in linear multi-agent systems," *IEEE Trans. Autom. Control*, vol. 59, no. 2, pp. 283–296, Feb. 2014.

[20] M. Lin, F. Fardad, and M. R. Jovanović, "Algorithms for leader selection in stochastically forced consensus networks," *IEEE Trans. Autom. Control*, vol. 59, no. 7, pp. 1789–1802, Jul. 2014.

[21] L. Xiao, S. Boyd, and S.-J. Kim, "Distributed average consensus with least-mean-square deviation," *J. Parallel Distrib. Comput.*, vol. 67, pp. 33–46, 2007.

[22] C. W. Wu, "Algebraic connectivity of directed graphs," *Linear Multilin. Alg.*, vol. 53, no. 3, pp. 203–223, 2005.

[23] R. Agaev and P. Chebotarev, "On the spectra of nonsymmetric Laplacian matrices," *Lin. Alg. Appl.*, vol. 399, pp. 157–168, 2005.

[24] L. Arnold, *Stochastic Differential Equations*. New York: Wiley, 1974.

[25] R. A. Horn and C. R. Johnson, *Matrix Analysis*. Cambridge, U.K.: Cambridge Univ. Press, 1985.

[26] I. Poulakakis, G. Young, L. Scardovi, and N. E. Leonard, "Node classification in networks of stochastic evidence accumulators," arXiv:1210.4235, Sep. 2014.

[27] M. E. J. Newman, *Networks: An Introduction*. Oxford, U.K.: Oxford Univ. Press, 2010.

[28] M. Woodbury, *Inverting Modified Matrices*. Princeton, NJ: Princeton University, 1950, ser. Memo. Rep. no. 42, Statistical Research Group.